

Architecture for high-sensitivity single-shot readout and control of the electron spin of individual donors in silicon

A. Morello,^{1,*} C. C. Escott,¹ H. Huebl,^{1,†} L. H. Willems van Beveren,¹ L. C. L. Hollenberg,² D. N. Jamieson,² A. S. Dzurak,¹ and R. G. Clark¹

¹ARC Centre of Excellence for Quantum Computer Technology, Schools of Electrical Engineering & Telecommunications and Physics, University of New South Wales, Sydney, New South Wales 2052, Australia

²ARC Centre of Excellence for Quantum Computer Technology, School of Physics, University of Melbourne, Melbourne, Victoria 3010, Australia

(Received 16 July 2009; published 14 August 2009)

We describe a method to control and detect in single shot the electron spin state of an individual donor in silicon with greatly enhanced sensitivity. A silicon-based single-electron transistor (SET) allows for spin-dependent tunneling of the donor electron directly into the SET island during the readout phase. Simulations show that the charge transfer signals are typically $\Delta q \geq 0.2e$ —over an order of magnitude larger than achievable with metallic SETs on the SiO₂ surface. A complete spin-based qubit structure is obtained by adding a local electron spin resonance line for coherent spin control. This architecture is ideally suited to demonstrate and study the coherent properties of donor electron spins, but can be expanded and integrated with classical control electronics in the context of scale up.

DOI: [10.1103/PhysRevB.80.081307](https://doi.org/10.1103/PhysRevB.80.081307)

PACS number(s): 73.23.Hk, 03.67.Lx, 71.55.Cn, 85.35.Gv

Electron spins bound to donor nuclei in silicon have exceptionally long coherence and relaxation times, relative to the time scale for the control of their quantum state,¹ and are thus a promising qubit system. The electron spin coherence time of a phosphorus donor is $T_2 > 60$ ms at $T = 6.9$ K in isotopically pure ²⁸Si,² already orders of magnitude longer than for GaAs quantum dot systems^{3,4} and still far from the theoretical limit (dominated by the ²⁹Si impurity fraction,⁵ which can be minimized through processing). However, a major obstacle to realizing a donor electron spin qubit in silicon⁶ is the difficulty of detecting the spin state for individual donors typically 10–20 nm below a SiO₂ interface.

The first proposals for donor spin readout involved spin-charge conversion^{7,8} through spin-dependent tunneling to a doubly occupied D⁻ donor state. The change in electrostatic potential caused by an electron can be detected by a single-electron transistor (SET) on the SiO₂ surface, as shown, e.g., in a double-donor well structure.⁹ The sensitivity of the detection scheme is quantified by the charge transfer signal $\Delta q/e$, defined as the relative shift in the SET bias point caused by the displacement of a nearby charge. $\Delta q/e = 1$ if an electron is removed from the SET island and taken to infinity. Clearly, $\Delta q/e < 1$ if the coupling between donor and SET is purely electrostatic, i.e., no charge can be directly transferred between the two. The exact value depends on how far the electron can move to/from or in the vicinity of the SET island: for a charge moving some 20 nm laterally in the silicon, 20 nm below the tip of the island of a surface SET, the signal is typically very small, $\Delta q/e \sim 0.01$. This fact has encouraged proposals in which $\Delta q/e$ can be increased by confining the donor electron close to the SiO₂ interface,¹⁰ thus closer to the SET. On the other hand, in quantum dot systems the successful readout of a single electron spin has been achieved by monitoring the spin-dependent tunneling of the electron into a reservoir.¹¹ Here we take this concept a step further and present a donor-based, electron spin qubit device, where the charge transfer signal upon spin readout can be increased by over an order of

magnitude as compared to previous proposals. Our architecture combines recently developed silicon quantum dot¹² and SET (Ref. 13) technologies with precise single-ion implantation¹⁴ and local electron spin resonance (ESR).^{4,15} The crucial feature of this device consists in using the island of a subsurface silicon SET as the electron reservoir for spin-dependent electron tunneling, greatly enhancing the charge signal. We show that this method allows fast (potentially in the nanosecond range) and high-sensitivity spin readout with no back action before the measurement, therefore protecting the qubit from decoherence due to the measurement setup.

A sketch of the proposed donor spin qubit device is shown in Fig. 1(a). It consists of three main elements: (i) a phosphorus donor, introduced in the intrinsic Si substrate by single-ion implantation;¹⁴ (ii) a Si-SET,^{12,13} fabricated next to the donor implant site, with a distance $d \sim 50$ nm between donor and SET island; and (iii) a coplanar transmission line, terminated by a short-circuit that runs just above the donor. The Si-SET comprises two aluminum barrier gates and an overlaying top gate, insulated by Al₂O₃ and deposited on high-quality SiO₂, typically 5 nm thick. The top gate extends to source/drain n⁺ doped regions, and induces an electron layer under the SiO₂ when biased to $V_{\text{top}} \geq 1$ V. Setting the barrier gate voltages to $V_{\text{B}1,2} < V_{\text{top}}$, the bottom of the conduction band can be lifted above the Fermi energy E_F , thereby interrupting the electron layer and forming the island of a SET [Fig. 1(b)].

The crucial difference between the Si-SET described here and the more common surface Al-SETs is that the SET island now consists of a small area of electron gas, electrostatically induced *under the SiO₂ layer*. Therefore, it is possible to construct a device where *an electron can tunnel between the donor and the island of the SET*. This feature gives a charge transfer signal an order of magnitude larger than achievable with other detection schemes, where the charge sensor is only electrostatically coupled to the qubit. In addition, the Si-SET has the advantage of being compatible with standard metal-oxide-semiconductor (MOS) fabrication processes

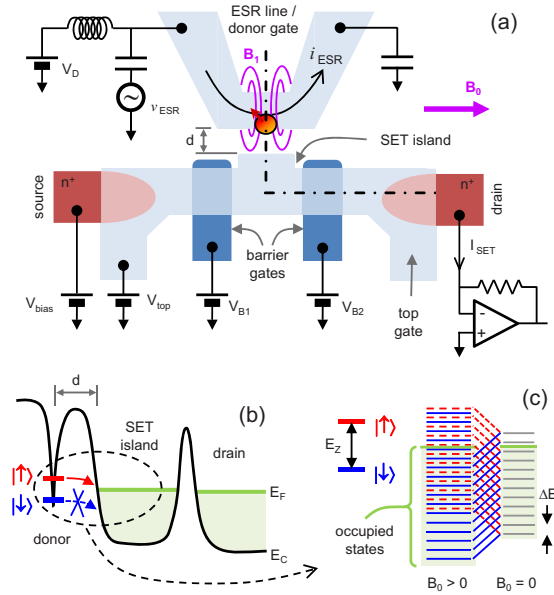


FIG. 1. (Color online) (a) Schematic top view of the spin qubit device. The donor-SET island distance is $d \sim 50$ nm. (b) Energy profile along the dash-dotted line in panel (a). The density of electron states in the SET island is approximated as a quasicontinuum. (c) In reality, the SET has a finite number of electrons: the quasicontinuum approximation and the spin readout method are valid as long as $\Delta E \ll E_Z$.

since it does not require shadow metal evaporation.

The shorted coplanar transmission line serves a double purpose: (i) it carries microwave pulses that produce an oscillating magnetic field, B_1 , for local ESR,⁴ and (ii) it acts as a dc gate for the electrostatic potential of the donor below it through application of a static voltage V_D . The ability to use a transmission line to perform local ESR of donor spins while simultaneously applying a dc bias was recently demonstrated by electrically detected magnetic resonance at $T \ll 1$ K.¹⁵ Since the transmission line is nonresonant, the structure is entirely broadband. The purpose of the short-circuit termination is to create a node of the electric field at the donor site, while having the maximum value of the current, i_{ESR} , for fast coherent manipulation of the spin state.⁴ If the short-circuit termination has a cross-section $\sim 100 \times 100$ nm², a Rabi π pulse can be obtained in < 100 ns with less than -30 dBm microwave power on the chip.

Figure 1(b) shows the energy profile along the dash-dotted line in Fig. 1(a). First we encounter the potential well created by the donor ion, which can bind one (D^0) or two (D^-) electrons. In the following we shall restrict our analysis to the one-electron D^0 state. By applying a static magnetic field B_0 in the plane of the chip, the energy of the $|\uparrow\rangle$ and $|\downarrow\rangle$ spin states is split by an amount $E_Z = 2g\mu_B B_0 S$, with $g \approx 2$ and $S = 1/2$. Proceeding further we enter the SET island, where the bottom of the conduction band E_C is pushed below the Fermi level E_F by the positive V_{top} . Between donor and SET is an energy barrier that allows electron tunneling at a rate Γ_D , mainly determined by the distance d (~ 50 nm) between donor and island. Turning toward the drain contact, we cross the tunnel barrier created by $V_{B2} < V_{top}$. This barrier is easily tunable to have a tunnel rate $\Gamma_{SET} \gg \Gamma_D$.

Spin-to-charge conversion is achieved by tuning

$\{V_D, V_{top}\}$ so that only the energy of the $|\uparrow\rangle$ state is above the electrochemical potential of a charge reservoir. The detection of a charge transfer from donor to reservoir then corresponds to the single-shot projective measurement of the $|\uparrow\rangle$ state, as demonstrated in GaAs quantum dots.¹¹ Here we propose to use the SET island as electron reservoir, instead of having a separate bulk electron layer. For this readout method to work, the Fermi distribution in the SET island must be sharp on the energy scale set by E_Z . This condition is abundantly fulfilled by cooling the system to $T \sim 100$ mK and using an operation frequency ~ 40 GHz for the ESR system, corresponding to $B_0 \approx 1.4$ T and $E_Z/k_B \approx 2$ K. In fact, due to the finite number of electrons, the density of states in the SET island is not a real continuum, but for the purpose of spin readout it is sufficient for the single-particle energy spacing, ΔE , to be much smaller than E_Z and comparable to $k_B T$ [Fig. 1(c)]. Taking an SET island of area $A = 50 \times 100$ nm², we estimate $\Delta E \sim 2\pi\hbar^2/gm^*A = 24$ μ eV ($g = 4$ is the spin + valley degeneracy and $m^* = 8.9 \times 10^{-31}$ kg is the effective mass), already smaller than the thermal broadening of the Fermi function at $T \sim 100$ mK.

The advantage of having an integrated charge sensor and electron reservoir is best appreciated by thinking of this architecture as a “parallel double quantum dot” configuration.¹⁶ We label the donor as “dot 1,” which can only have 0 or 1 electrons, and the SET island as “dot 2,” with a large number of electrons $N, N+1, \dots$ and charging energy $E_{C2} \sim 1$ meV.¹³ The charging energy of the donor is $E_{C1} \sim 30\text{--}40$ meV, depending on the capacitance to its surroundings.¹⁷ Dot 2 is connected to source and drain contacts and can be measured in transport, while the charge state of dot 1 can only be changed by electron tunneling to or from dot 2.

For two quantum dots with mutual coupling energy E_m , the electrochemical potential of one dot depends on the charge state of the other.¹⁸ Therefore the SET can have two ladders of electrochemical potentials, shifted by E_m with respect to each other, depending on the charge state of the donor. The donor states are split by $E_Z = \mu_1(1_\uparrow, N) - \mu_1(1_\downarrow, N)$. In Fig. 2(a) we sketch a situation where the charge state of the “double dot” is $(1, N)$ (the donor is neutral), thus the relevant electrochemical potentials on the SET side are the solid lines, $\mu_2(1, N), \mu_2(1, N+1), \dots$ and the corresponding $\{V_D, V_{top}\}$ point in Fig. 2(b) is given by the dashes labeled $|\downarrow\rangle, |\uparrow\rangle$. The SET is thus in Coulomb blockade, with $I_{SET} = 0$, because $\mu_2(1, N+1)$ is far above the Fermi level in the source/drain contacts.

Next we wish to lift μ_1 by decreasing V_D , while keeping the μ_2 ladder fixed and $\mu_2(0, N+1)$ in the source/drain bias window. Because of cross capacitance, this requires a compensating V_{top} to keep the operation point $\{V_D, V_{top}\}$ along the solid line in Fig. 2(b). When $\mu_1(1, N) > \mu_2(0, N+1)$, the donor electron can tunnel onto the SET island (at a rate Γ_D) and out to the drain (at a rate $\Gamma_{SET} \gg \Gamma_D$), leaving behind a positive charge at the donor site. This charge “pulls down” the ladder of electrochemical potentials for the SET, now represented by the dashed lines in Fig. 2(a), $\mu_2(0, N), \mu_2(0, N+1), \dots$ and since $\mu_2(0, N+1)$ is in the source-drain bias window, I_{SET} jumps to its maximum value. The charge transfer signal is $\Delta q/e = \Delta V_m / \Delta V_{C2}$ [Fig. 2(b)], i.e., the shift of the

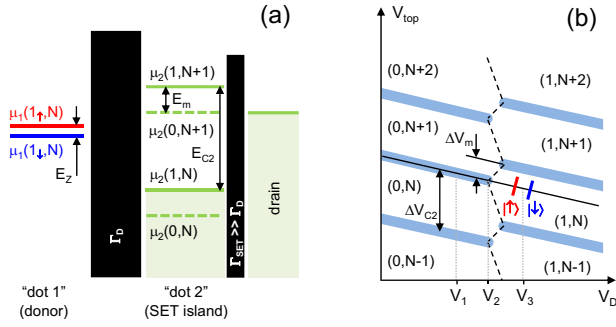


FIG. 2. (Color online) (a) Sketch of the electrochemical potentials in the “parallel double dot” picture. The relevant SET potentials are the solid lines when the donor is neutral (D^0 state) or the dashed lines when the donor is ionized (D^+ state). (b) Charge stability diagram in the double dot picture. The broad lines represent the SET current peaks, $I_{\text{SET}} > 0$, spaced by $\Delta V_{C2} = E_{C2}/e\alpha_2$ along the V_{top} axis, where α_2 is the lever arm between top gate and SET island. The dashes labeled $|\uparrow\rangle$, $|\downarrow\rangle$ represent the positions of $\mu_1(1_{\uparrow}, N)$ and $\mu_1(1_{\downarrow}, N)$ as given in panel (a). The μ_2 ladder can be kept fixed by moving $\{V_D, V_{\text{top}}\}$ along the thin black line.

SET Coulomb peaks due to the ionization of the donor, divided by their period. Note that $\Delta q/e$ is exactly what would be obtained by moving a positive charge from infinity to the donor site. Thus, $\Delta q/e \rightarrow 1$ as the donor location approaches the SET island.

We have set up a device model, shown in Figs. 3(a) and 3(b), for use in the boundary-element capacitance extraction code FASTCAP (Ref. 19) to determine coupling capacitances as a function of donor position. In the model the gates and electron layers are described by metallic conductors of the appropriate size and the donor is represented as a metal cube with sides of length $2a_B$ ($a_B \approx 2.5$ nm is the Bohr radius in silicon). $\Delta q/e$ can be expressed as the ratio $C_m/C_{1\Sigma}$, where C_m is the mutual capacitance between donor and SET island, and $C_{1\Sigma}$ is the total donor capacitance. Figure 3(c) shows the resulting $\Delta q/e$, assuming 50 nm gap between top gate and ESR line, 5 nm SiO_2 thickness, and donor in the y - z plane. For a donor right under the tip of the ESR line, and 15 nm below the Si/SiO_2 interface, we find $\Delta q/e \sim 0.2$. With $E_{C2} \sim 1$ meV and $T \sim 100$ mK, I_{SET} can shift from zero to its maximum value, I_{max} .

A typical spin control and readout sequence would pro-

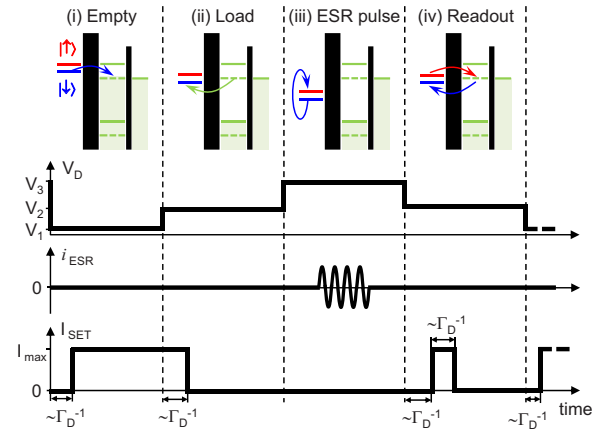


FIG. 4. (Color online) Pulsing protocol and corresponding SET signal for the coherent control and readout of a donor electron spin. The donor gate voltages $V_{1,2,3}$ are shown also in Fig. 2(b).

ceed as shown in Fig. 4, always assuming the μ_2 ladder is kept fixed by using compensated $\{V_D, V_{\text{top}}\}$ pulses. (i) Empty: the donor is ionized when $V_D = V_1$, causing $\mu_1(1_{\downarrow}, N) > \mu_2(0, N+1)$. The successful donor ionization is signaled by $I_{\text{SET}} = I_{\text{max}}$. (ii) Load: a new electron is loaded into the ground Zeeman state $|\downarrow\rangle$, by choosing V_2 such that $\mu_1(1_{\uparrow}, N) > \mu_2(0, N+1) > \mu_1(1_{\downarrow}, N)$, and $I_{\text{SET}} = 0$. (iii) ESR pulse: when $V_D = V_3$ both donor levels are far below $\mu_2(0, N+1)$. The spin undergoes coherent Rabi rotations under the effect of microwave pulses applied to the ESR line. Here we take the example of a π -pulse where the final state is $|\uparrow\rangle$. (iv) Readout: $V_D = V_2$, and since $\mu_1(1_{\uparrow}, N) > \mu_2(0, N+1)$, the electron in the $|\uparrow\rangle$ state tunnels off the donor into the SET island, unblocking the conduction. However, since $\mu_2(0, N+1) > \mu_1(1_{\downarrow}, N)$, another electron can tunnel onto the donor in the state $|\downarrow\rangle$, blocking the SET again. Thus, an electron in $|\uparrow\rangle$ is signaled by a “blip” in I_{SET} , with a duration of order Γ_D^{-1} . The inhomogeneous spin coherence time, T_2^* , can be extracted by observing the decay of Rabi oscillations, obtained by counting the occurrence of $|\uparrow\rangle$ states as a function of ESR pulse duration. The spin-lattice relaxation time, T_1 , can be obtained by loading an electron in an unknown state, i.e., using $V_D = V_3$ for the load pulse, then counting the occurrence of $|\uparrow\rangle$ states as a function of the waiting time between load and measurement¹¹ (no ESR required).

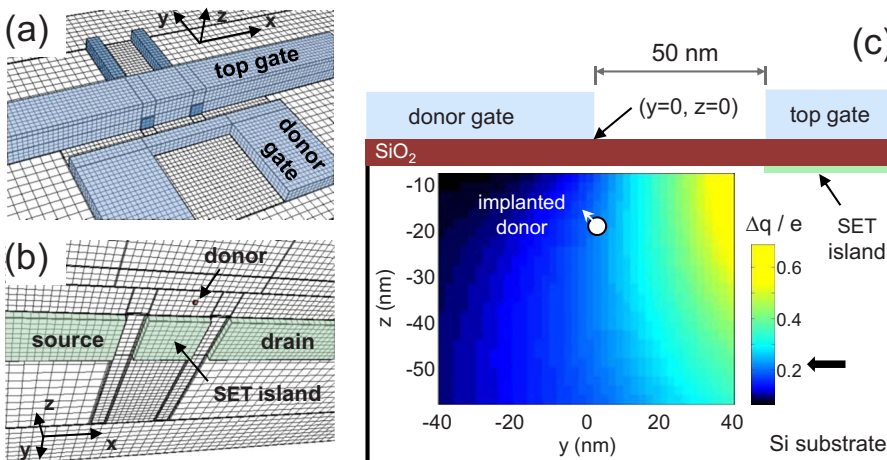


FIG. 3. (Color online) (a) Top and (b) bottom view of the device model used to calculate the charge transfer signal $\Delta q/e$. Filled areas represent gates and electron layers as indicated. (c) FASTCAP calculation of $\Delta q/e$ as a function of donor position in the y - z plane. We used a mesh five times finer than shown by the thin lines in (a) and (b), yielding discretization errors $< 5\%$ of the $\Delta q/e$ value at each point. For a donor under the tip of the donor gate, 15 nm below the Si/SiO_2 interface, $\Delta q/e \approx 0.2$ (black arrow).

An important feature of our device is that, due to Coulomb blockade, $I_{\text{SET}}=0$ for the whole time the electron resides on the donor, i.e., the charge sensor is automatically switched off. The type of back action arising, e.g., from the current through a quantum point contact used as charge sensor,²⁰ is therefore eliminated.

The time scale for projective readout of the qubit is set by the typical tunneling time between donor and SET island, Γ_D^{-1} . In the design discussed here, Γ_D is exponentially sensitive to d , but some level of control could be achieved by introducing an additional gate between ESR line and SET. However we note that the acceptable range of Γ_D for reliable spin readout is extremely wide. The upper bound to Γ_D^{-1} is set by the spin-lattice relaxation time, T_1 , since an electron in the $|\uparrow\rangle$ state must be measured before it decays to $|\downarrow\rangle$. The bulk value for P in Si is $T_1 \approx 3000$ s at $T=1.25$ K, further increasing as $1/T$.²¹ For a donor placed near a Si/SiO₂ interface, paramagnetic defects and charge traps may give an additional contribution to the spin relaxation and dephasing.²² However, this contribution vanishes exponentially when $k_B T \ll E_Z$ due to high spin polarization.²³ The lower bound to Γ_D^{-1} is simply set by the bandwidth of the circuit that detects I_{SET} . Here we note that an ideal readout scheme would exploit the fact that our system effectively provides a digital

signal ($I_{\text{SET}}=0$ or I_{max}) by connecting the SET to a cryogenic current comparator.²⁴ This method could yield the ultimate readout speed, potentially as fast as ~ 1 ns. The MOS compatibility of our design is significant, because it allows the on-chip integration of qubit devices and ultrafast cryogenic readout electronics, using the same industry-standard fabrication process. This is extremely advantageous both for readout speed—minimizing the capacitance of the interconnects—and for the scale up of a quantum computer.

In conclusion, we have shown that recently developed Si-SET technology^{12,13} can be harnessed to create a compact donor spin qubit architecture, wherein the island of the SET is used as a reservoir for high-sensitivity spin readout. The compatibility with MOS fabrication techniques is very advantageous to integrate the qubits with digital on-chip electronics²⁴ and achieve the ultimate in readout speed and sensitivity for spins in the solid state. This architecture removes a major impediment to exploiting the natural advantages of donors in silicon as a platform for scalable qubit science.

This work was funded by the Australian Research Council, the Australian Government, the U.S. National Security Agency, and the U.S. Army Research Office under Contract No. W911NF-08-1-0527.

*a.morello@unsw.edu.au

[†]Present address: Walther-Meißner-Institut, Bayerische Akademie der Wissenschaften, 85748 Garching, Germany.

¹C. D. Hill, L. C. L. Hollenberg, A. G. Fowler, C. J. Wellard, A. D. Greentree, and H.-S. Goan, *Phys. Rev. B* **72**, 045350 (2005).

²A. M. Tyryshkin, S. A. Lyon, A. V. Astashkin, and A. M. Raitsimring, *Phys. Rev. B* **68**, 193207 (2003).

³J. R. Petta, A. C. Johnson, J. M. Taylor, E. A. Laird, A. Yacoby, M. D. Lukin, C. M. Marcus, M. P. Hanson, and A. C. Gossard, *Science* **309**, 2180 (2005).

⁴F. H. L. Koppens, C. Buizert, K. J. Tielrooij, I. T. Vink, K. C. Nowack, T. Meunier, L. P. Kouwenhoven, and L. M. K. Vandersypen, *Nature (London)* **442**, 766 (2006).

⁵W. M. Witzel, R. de Sousa, and S. Das Sarma, *Phys. Rev. B* **72**, 161306(R) (2005).

⁶R. Vrijen, E. Yablonovitch, K. Wang, H. W. Jiang, A. Balandin, V. Roychowdhury, T. Mor, and D. DiVincenzo, *Phys. Rev. A* **62**, 012306 (2000); L. C. L. Hollenberg, A. D. Greentree, A. G. Fowler, and C. J. Wellard, *Phys. Rev. B* **74**, 045311 (2006).

⁷B. E. Kane, *Nature (London)* **393**, 133 (1998).

⁸L. C. L. Hollenberg, C. J. Wellard, C. I. Pakes, and A. G. Fowler, *Phys. Rev. B* **69**, 233301 (2004).

⁹S. E. S. Andresen, R. Brenner, C. J. Wellard, C. Yang, T. Hopf, C. C. Escott, R. G. Clark, A. S. Dzurak, D. N. Jamieson, and L. C. L. Hollenberg, *Nano Lett.* **7**, 2000 (2007).

¹⁰M. J. Calderon, B. Koiller, X. Hu, and S. Das Sarma, *Phys. Rev. Lett.* **96**, 096802 (2006).

¹¹J. M. Elzerman, R. Hanson, L. H. Willems van Beveren, B. Witkamp, L. M. K. Vandersypen, and L. P. Kouwenhoven, *Nature (London)* **430**, 431 (2004).

¹²S. J. Angus, A. J. Ferguson, A. S. Dzurak, and R. G. Clark, *Nano Lett.* **7**, 2051 (2007).

¹³S. J. Angus, A. J. Ferguson, A. S. Dzurak, and R. G. Clark, *Appl.*

Phys. Lett. **92**, 112103 (2008).

¹⁴D. N. Jamieson, C. Yang, T. Hopf, S. M. Hearne, C. I. Pakes, S. Prawer, M. Mitic, E. Gauja, S. E. Andresen, F. E. Hudson, A. S. Dzurak, and R. G. Clark, *Appl. Phys. Lett.* **86**, 202101 (2005).

¹⁵L. H. Willems van Beveren, H. Huebl, D. R. McCamey, T. Duty, A. J. Ferguson, R. G. Clark, and M. S. Brandt, *Appl. Phys. Lett.* **93**, 072102 (2008).

¹⁶F. Hofmann, T. Heinzl, D. A. Wharam, J. P. Kotthaus, G. Böhm, W. Klein, G. Tränkle, and G. Weimann, *Phys. Rev. B* **51**, 13872 (1995).

¹⁷G. P. Lansbergen, R. Rahman, C. J. Wellard, I. Woo, J. Caro, N. Collaert, S. Biesemans, G. Klimeck, L. C. L. Hollenberg, and S. Rogge, *Nat. Phys.* **4**, 656 (2008); K. Tan, K. Chan, M. Mötönen, A. Morello, C. Yang, J. van Donkelaar, A. Alves, J. Pirkkalainen, D. Jamieson, R. Clark, and A. Dzurak, arXiv:0905.4358 (unpublished).

¹⁸W. G. van der Wiel, S. De Franceschi, J. M. Elzerman, T. Fujisawa, S. Tarucha, and L. P. Kouwenhoven, *Rev. Mod. Phys.* **75**, 1 (2003).

¹⁹K. Nabors and J. White, *IEEE Trans. Comput.-Aided Des.* **10**, 1447 (1991).

²⁰S. Gustavsson, M. Studer, R. Leturcq, T. Ihn, K. Ensslin, D. C. Driscoll, and A. C. Gossard, *Phys. Rev. Lett.* **99**, 206804 (2007); D. Taubert, M. Pioro-Ladriere, D. Schroer, D. Harbusch, A. S. Sachrajda, and S. Ludwig, *ibid.* **100**, 176805 (2008).

²¹G. Feher and E. A. Gere, *Phys. Rev.* **114**, 1245 (1959).

²²T. Schenkel, J. A. Little, A. Persaud, A. M. Tyryshkin, S. A. Lyon, R. de Sousa, K. B. Whaley, J. Bokor, J. Shangkuan, and I. Chakarov, *Appl. Phys. Lett.* **88**, 112101 (2006).

²³R. de Sousa, *Phys. Rev. B* **76**, 245306 (2007).

²⁴T. Gurrieri, M. Carroll, M. Lilly, and J. Levy, NANO'08, 8th IEEE Conference on Nanotechnology, Arlington, TX, 18–21 August 2008, p. 609.